ISSN 0021-3640, JETP Letters, 2008, Vol. 87, No. 1, pp. 39–44. © Pleiades Publishing, Ltd., 2008.
Original Russian Text © A.M. Kadomtseva, Yu.F. Popov, G.P. Vorob'ev, A.A. Mukhin, V.Yu. Ivanov, A.M. Kuz'menko, L.N. Bezmaternykh, 2008, published in Pis'ma v Zhurnal Éksperimental'noĭ i Teoreticheskoĭ Fiziki, 2008, Vol. 87, No. 1, pp. 45–50.

Influence of the Ground State of the Pr^{3+} Ion on Magnetic and Magnetoelectric Properties of the $PrFe_3(BO_3)_4$ Multiferroic

A. M. Kadomtseva[a], Yu. F. Popov[a], G. P. Vorob'ev[a], A. A. Mukhin[b], V. Yu. Ivanov[b], A. M. Kuz'menko[b], and L. N. Bezmaternykh[c]
[a] *Moscow State University, Moscow, 119992 Russia*
e-mail: kadomts@plms.ru
[b] *Prokhorov Institute of General Physics, Russian Academy of Sciences, Moscow, 119991 Russia*
[c] *Institute of Physics, Siberian Branch, Russian Academy of Sciences, Krasnoyarsk, 660038 Russia*

Received November 9, 2007; in final form, November 19, 2007

The magnetic, magnetoelectric, and magnetoelastic properties of a $PrFe_3(BO_3)_4$ single crystal and the phase transitions induced in this crystal by the magnetic field are studied both experimentally and theoretically. Unlike the previously investigated ferroborates, this material is characterized by a singlet ground state of the rare-earth ion. It is found that, below $T_N = 32$ K, the magnetic structure of the crystal in the absence of the magnetic field is uniaxial ($\mathbf{l} \parallel \mathbf{c}$), while, in a strong magnetic field $\mathbf{H} \parallel \mathbf{c}$ ($H_{cr} \sim 43$ kOe at $T = 4.2$ K), a Fe^{3+} spin reorientation to the basal plane takes place. The reorientation is accompanied by anomalies in magnetization, magnetostriction, and electric polarization. The threshold field values determined in the temperature interval 2–32 K are used to plot an H–T phase diagram. The contribution of the Pr^{3+} ion ground state to the parameters under study is revealed, and the influence of the praseodymium ion on the magnetic and magnetoelectric properties of praseodymium ferroborate is analyzed.

PACS numbers: 75.80.+q

DOI: 10.1134/S0021364008010104

INTRODUCTION

In the last few years, the interest in studying the $RFe_3(BO_3)_4$ rare-earth ferroborates, whose crystal structure is described by the $R32$ (D_3^7) space group, has quickened (see review [1]). Interest is primarily caused by the remarkable magnetic properties of these materials: a rare-earth ferroborate contains two interacting magnetic subsystems, namely, the iron subsystem and the rare-earth one. In addition, it was recently found that rare-earth ferroborates belong to a new class of multiferroics [2–4]. The magnetic and magnetoelectric properties of these compounds widely vary depending on the ground state of the rare-earth ion [5]. For example, neodymium, gadolinium, and terbium ferroborates, which have the rare ion ground states $^4I_{9/2}$, $^8S_{7/2}$, and $^7F_6$, respectively, have different magnetic structures below the Néel temperature T_N: $NdFe_3(BO_3)_4$ has an easy-plane structure, $TbFe_3(BO_3)_4$ has an easy-axis structure, and $GdFe_3(BO_3)_4$ has an easy-axis structure at temperatures $T < 10$ K and an easy-plane structure in the temperature interval $10\ K < T < T_N$. The maximum electric polarization induced by the magnetic field is observed for $NdFe_3(BO_3)_4$, and the minimum one is observed for $TbFe_3(BO_3)_4$, where the Tb^{3+} ion is strongly anisotropic (an Ising ion) and, because of the specificity of the ground state, makes virtually no contribution to electric polarization. It is of special interest to study the magnetic and magnetoelectric interactions in praseodymium ferroborate, $PrFe_3(BO_3)_4$, in which the Pr^{3+} ion is of a non-Kramers and virtually singlet character (the $^3H_4$ ground state). The fact that the properties of $PrFe_3(BO_3)_4$ are rather poorly investigated makes this study still more topical.

EXPERIMENT

We carried out comprehensive studies of magnetic, magnetoelastic, and magnetoelectric properties of $PrFe_3(BO_3)_4$ single crystals in the temperature interval from 2 to 300 K. The praseodymium ferroborate single crystals were grown by the solution-melt technique (a detailed description of the synthesis is given in [6]). Magnetic properties were measured in a static magnetic field by an MPMS-50 SQUID magnetometer and in a pulsed magnetic field of up to 250 kOe by the induction method using differential coils. Magnetostriction was measured by contact piezoelectric sensors, and electric polarization was determined by measuring the electric charge induced in the sample by the pulsed magnetic field.

Figure 1 shows the temperature dependence of the magnetic susceptibility measured in the constant magnetic field $H \sim 1$ kOe by the SQUID magnetometer in the temperature interval 2–300 K. As the temperature

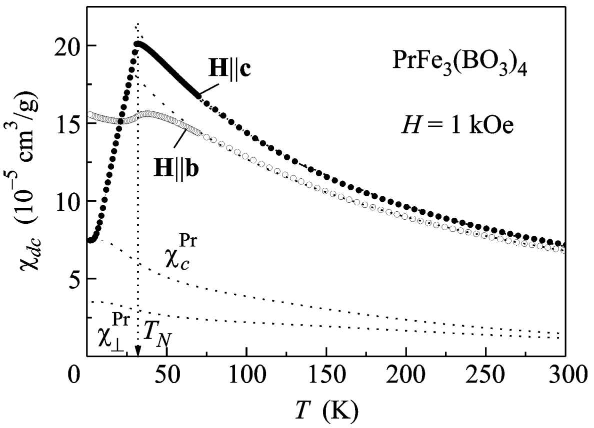

Fig. 1. Temperature dependences of magnetic susceptibility measured in a field of 1 kOe for the field orientations along the *c* and *b* axes. The circles represent the experimental data, and the dotted lines represent the calculation that allows the separation of the rare-earth susceptibility component (see the main body of the paper).

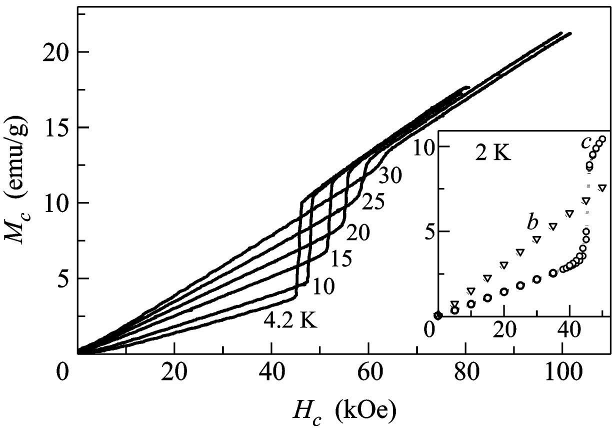

Fig. 2. Magnetization curves of the $PrFe_3(BO_3)_4$ crystal along the *c* axis: measurements in pulsed magnetic fields for different temperatures. The inset shows the magnetization curves measured at $T = 2.0$ K along the *c* and *b* axes by the SQUID magnetometer.

decreases from 300 K to $T_N = 32$ K, the susceptibility along the *c* axis exhibits a smooth growth; upon a further temperature decrease, χ_c sharply drops from 2×10^{-4} cm^3/g at T_N to 0.75×10^{-4} cm^3/g at $T = 2$ K. The susceptibility along the *b* axis, χ_b, smoothly increases as the temperature decreases from 300 K to T_N and is virtually temperature independent below T_N. The behavior of the susceptibility χ_c indicates that, below T_N, the spins of the Fe^{3+} ions are ordered along the *c* axis and cause an antiferromagnetic polarization of the Pr^{3+} ions due to the Pr–Fe exchange interaction. The magnetization curves obtained for $PrFe_3(BO_3)_4$ magnetization along the *c* axis in the static (see the inset in Fig. 2) and the pulsed magnetic fields (Fig. 2) exhibit abrupt jumps due to the Fe^{3+} spin reorientation from the *c* axis to the basal plane with the accompanying change in the orientation of the magnetic moments of the Pr^{3+} ions. The magnetic field corresponding to this transition is equal to ~45 kOe at 4.2 K and increases to 63 kOe as the temperature increases to 30 K. It should be noted that the magnetization jumps were only observed for the magnetization curves measured in the magnetic field **H || c**. This fact suggests that the spins of the Fe^{3+} ions are oriented along the *c* axis in the absence of the field and that their reorientation can occur only in a sufficiently high magnetic field exceeding a certain threshold.

The process of the spin reorientation induced by the field **H || c** was accompanied by jumps in magnetostrictive strains (Fig. 3). The threshold fields corresponding to the jumps in the magnetization and in the magnetostriction correlate with each other. We note that the magnetostrictive strains were relatively small and reached ~5×10^{-6}.

It was also found that the spin reorientation transition induced by magnetic field **H || c** was accompanied by anomalies in electric polarization in the form of small "peaks" (Fig. 4). The magnitude and shape of the polarization anomalies is governed (as it will be shown below) by the inevitable small deviation of the field from the strict orientation along the *c* axis toward the basal plane. The minimum amplitude of the peaks was observed along the *c* axis, $\Delta P_c(H_c)$; according to the symmetry analysis (see [3]), the latter quantity, in contrast to $\Delta P_{a,\,b}(H_c)$, is determined by the term of the fourth order in the antiferromagnetic vector **l**.

The longitudinal electric polarization in the basal plane exhibited a quadratic dependence on the magnetic field along the *a* and *b* axes of the crystal (Fig. 5) without any anomalies indicating the presence of a phase transition in the magnetic field, in contrast to the case of **H || c**.

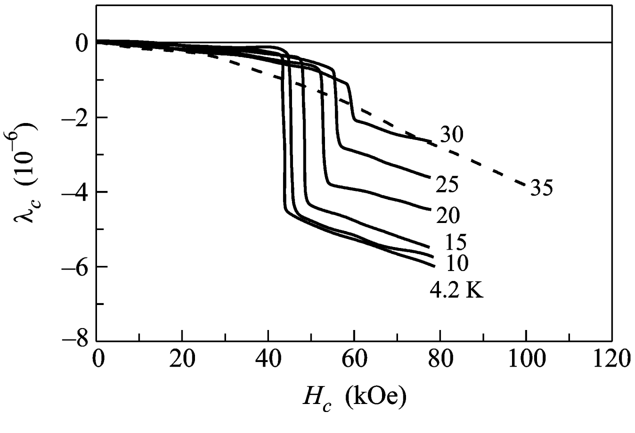

Fig. 3. Field dependences of the longitudinal magnetostriction along the *c* axis for different temperatures.

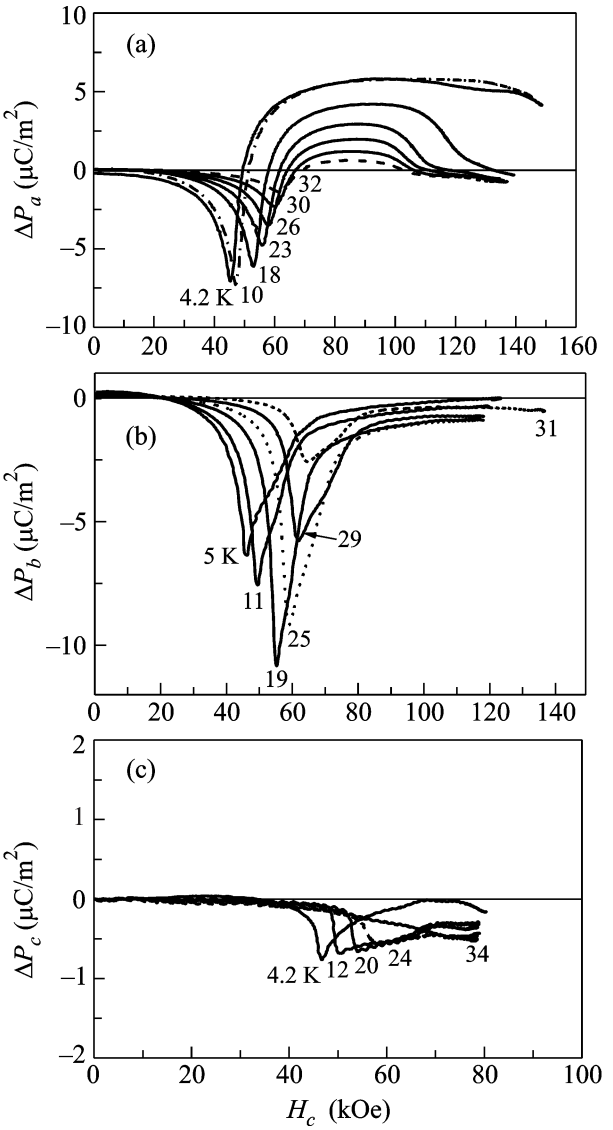

Fig. 4. Polarization jumps along the (a) *a*, (b) *b*, and (c) *c* axes versus the magnetic field applied along the *c* axis. The respective temperatures *T* are indicated near the curves.

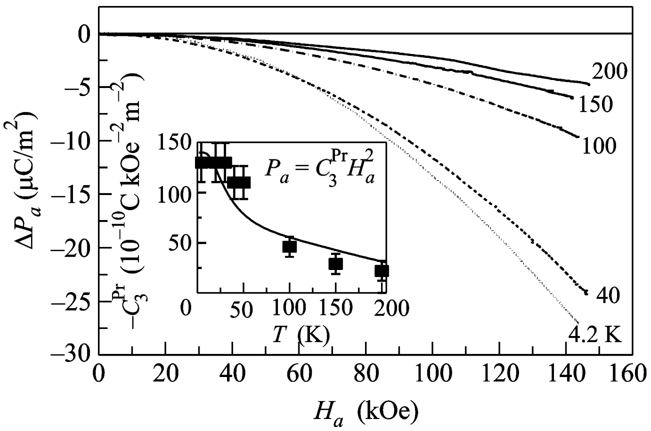

Fig. 5. Polarization jump along the *a* axis versus the magnetic field applied along the *a* axis for different temperatures. The inset shows the temperature dependence of the coefficient multiplying the term quadratic in the field: the squares represent the experimental data, and the curve represents the theoretical dependence.

Figure 6 shows the phase diagram $H(T)$ obtained from the measurements of the magnetic $M_C(H_C)$, magnetoelastic $\lambda_c(H_c)$, and magnetoelectric $\Delta P_{a,\,c}(H_c)$ properties of $\mathrm{PrFe_3(BO_3)_4}$. The diagram demonstrates a good agreement between the values of the threshold fields observed in different measurements.

THEORY AND DISCUSSION

For describing the magnetic properties of $\mathrm{PrFe_3(BO_3)_4}$ observed in the experiment, including the uniaxial antiferromagnetic structure, it is necessary to take into account the anisotropy introduced by the rare-earth subsystem. This factor is of fundamental importance, because the magnetic anisotropy of the Fe subsystem stabilizes the easy-plane state, as evidenced by the data on the $\mathrm{YFe_3(BO_3)_4}$ ferroborate with nonmagnetic $\mathrm{Y^{3+}}$ ions [7, 8]. According to our experimental data (Fig. 1), the maximum magnetic susceptibility of $\mathrm{Pr^{3+}}$ ions is observed along the *c* axis, which allows the stabilization of the uniaxial state in the presence of a sufficiently strong Pr–Fe exchange interaction. Another important feature of $\mathrm{PrFe_3(BO_3)_4}$ is the linear behavior of the experimental magnetization curves in both the uniaxial state and the spin-flop phase (Fig. 2). This feature points to a singlet character of the ground state of the non-Kramers $\mathrm{Pr^{3+}}$ ion in the crystal field: the ground state is separated by a sufficiently large energy gap from the superior energy levels. This leads to the absence of the magnetization saturation for the rare-earth subsystem in magnetic fields of up to 200 kOe, in contrast to the case of ferroborates containing $\mathrm{Tb^{3+}}$ Ising ions [4].

The magnetization of the two Pr sublattices can be represented in the form $m^{\pm} \approx \hat{\chi}^{\mathrm{Pr}}(T)\mathbf{H}^{\pm}_{\mathrm{eff}}$, where $\hat{\chi}^{\mathrm{Pr}}(T)$ is the magnetic susceptibility tensor of $\mathrm{Pr^{3+}}$ ions in the crystal field, $\mathbf{H}^{\pm}_{\mathrm{eff}} = \mathbf{H} + \mathbf{H}^{\pm}_{\mathrm{ex}}$ is the effective field, $\mathbf{H}^{\pm}_{\mathrm{ex}} \approx \pm(\lambda_{\perp}l_x,\ \lambda_{\perp}l_y,\ \lambda_z l_z)$ is the exchange field determined by the Pr–Fe interaction, $\mathbf{l} = (l_x,\ l_y,\ l_z)$ is the dimensionless antiferromagnetic vector of the Fe subsystem, and the ± signs corresponds to the two Pr sublattices. The total free energy of the whole system can be represented as

$$\Phi(\mathbf{l},\mathbf{H}) = -\frac{1}{2}\chi_{\perp}^{\mathrm{Fe}}\mathbf{H}^2 + (\chi_{\perp}^{\mathrm{Fe}} - \chi_{\parallel}^{\mathrm{Fe}})(\mathbf{H}\mathbf{l})^2$$

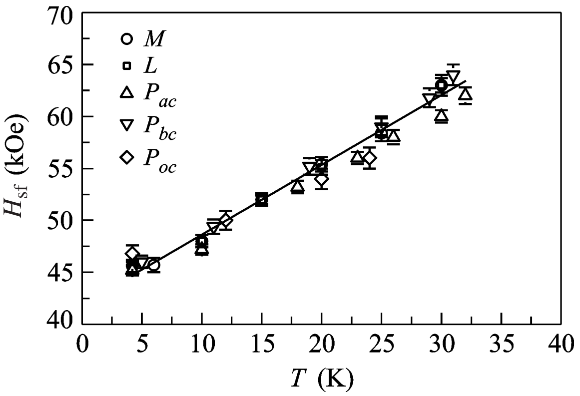

Fig. 6. Temperature dependence of the critical magnetic field determined from the magnetization, magnetostriction, and electric polarization measurements.

$$+\frac{1}{2}K_{\mathrm{Fe}}l_z^2-\frac{1}{4}\sum_{\alpha=\pm}\mathbf{H}^{\alpha}_{\mathrm{eff}}\hat{\chi}^{\mathrm{Pr}}\mathbf{H}^{\alpha}_{\mathrm{eff}} \tag{1}$$

$$=-\frac{1}{2}\chi_{\perp}^{\mathrm{Fe}}\mathbf{H}^2+(\chi_{\perp}^{\mathrm{Fe}}-\chi_{\parallel}^{\mathrm{Fe}})(\mathbf{H}\mathbf{l})^2+\frac{1}{2}K_{\mathrm{eff}}l_z^2$$

$$-\frac{1}{2}\chi_z^{\mathrm{Pr}}H_z^2-\frac{1}{2}\chi_{\perp}^{\mathrm{Pr}}(H_x^2+H_y^2)+\mathrm{const},$$

where the first three terms in the upper part describe the contribution of the antiferromagnetically ordered Fe subsystem and the last term describes the contribution of the rare-earth ions; $\chi_{\perp}^{\mathrm{Fe}}$ and $\chi_{\parallel}^{\mathrm{Fe}}$ are the transverse and longitudinal susceptibilities of the Fe subsystem ($\chi_{\parallel}^{\mathrm{Fe}} \longrightarrow 0$ as $T \longrightarrow 0$), respectively; χ_z^{Pr} and $\chi_{\perp}^{\mathrm{Pr}}$ are the magnetic susceptibility components of the Pr subsystem that are parallel to the c axis and perpendicular to it, respectively; $K_{\mathrm{Fe}} > 0$ is the uniaxial anisotropy constant of the Fe subsystem; and $K_{\mathrm{eff}} = K_{\mathrm{Fe}} - (\chi_z^{\mathrm{Pr}}\lambda_z^2 - \chi_{\perp}^{\mathrm{Pr}}\lambda_{\perp}^2)$ is the effective uniaxial anisotropy constant of the crystal with allowance for the anisotropic contribution of the Pr^{3+} ions and the Pr–Fe interaction. The negative rare-earth contribution $-(\chi_z^{\mathrm{Pr}}\lambda_z^2 - \chi_{\perp}^{\mathrm{Pr}}\lambda_{\perp}^2)$ to K_{eff} stabilizes the uniaxial state, and, at $K_{\mathrm{eff}} < 0$, it determines the field corresponding to the spin-flop transition in the case of $H \parallel c$: $H_{\mathrm{sf}} = [-K_{\mathrm{eff}}/(\chi_{\perp}^{\mathrm{Fe}} - \chi_{\parallel}^{\mathrm{Fe}})]^{1/2}$.

For the field H parallel to the c axis, from Eq. (1), it follows that the magnetization of the system is linear in the magnetic field in both the uniaxial state, $M_z = (\chi_{\parallel}^{\mathrm{Fe}} + \chi_z^{\mathrm{Pr}})H_z$ for $H_z < H_{\mathrm{sf}}$, and the spin-flop phase $M_z = (\chi_{\perp}^{\mathrm{Fe}} + \chi_z^{\mathrm{Pr}})H_z$ for $H_z > H_{\mathrm{sf}}$. This result agrees well with the experiment. The amplitude of the magnetization jump at the spin-flop transition at low temperatures is determined by the simple relation $\Delta M_z = \chi_{\perp}^{\mathrm{Fe}} H_{\mathrm{sf}}$, which yields a jump amplitude close to the experiment: ~5.6 G cm^3/g. This estimate was obtained by using the value of $\chi_{\perp}^{\mathrm{Fe}}$ determined for $\mathrm{YFe_3(BO_3)_4}$ in [7] ($\approx 0.125 \times 10^{-3}$ cm^3/g).

As noted above, the uniaxial state of $\mathrm{PrFe_3(BO_3)_4}$ is stabilized by the anisotropic contribution of the Pr^{3+} ions and the Pr–Fe interaction. At low temperatures, where $\chi_{\parallel}^{\mathrm{Fe}} \approx 0$, the magnetic susceptibility of the Pr subsystem along the c axis is directly determined by the measured susceptibility at $H = 0$ and, according to Fig. 1, is equal to $\chi_{z0}^{\mathrm{Pr}} = 0.75 \times 10^{-4}$ cm^3/g. The susceptibility of the Pr subsystem in the direction perpendicular to the c axis can be estimated as $\chi_{\perp 0}^{\mathrm{Pr}} = \chi_{\perp}^{\mathrm{exp}}(4.2\ \mathrm{K}) - \chi_{\perp}^{\mathrm{Fe}} \approx 0.35 \times 10^{-4}$ cm^3/g by using the known value of $\chi_{\perp}^{\mathrm{Fe}}$ for $\mathrm{YFe_3(BO_3)_4}$. Then, we can estimate the effective exchange field produced at the Pr^{3+} ions by the Fe subsystem:

$$H_{\mathrm{ex}}(\mathrm{Pr{-}Fe}) = \lambda_{\perp, z}$$

$$= [(K_{\mathrm{Fe}} + \chi_{\perp}^{\mathrm{Fe}}H_{\mathrm{sf}}^2)/(\chi_{z0}^{\mathrm{Pr}} - \chi_{\perp 0}^{\mathrm{Pr}})]^{1/2} \approx 115\ \mathrm{kOe}. \tag{2}$$

Here, we ignored the anisotropy of the Pr–Fe exchange and, for K_{Fe}, we used a value of 2.9×10^5 erg/g taken from the antiferromagnetic resonance data obtained for $\mathrm{YFe_3(BO_3)_4}$ [7].

To get an idea of the structure of the Pr^{3+} ion spectrum in the crystal field, we modeled the temperature dependences of the magnetic susceptibility (Fig. 1) in the paramagnetic region by representing the susceptibility as the sum of the contributions of the Fe and Pr subsystems:

$$\chi_{\alpha}(T) = C_{\mathrm{Fe}}/(T - \theta_{\mathrm{Fe}}) + \chi_{\alpha}^{\mathrm{Pr}}(T),$$

$$\chi_{\alpha}^{\mathrm{Pr}}(T) = [\chi_{\alpha 01}^{\mathrm{Pr}}(1 - e^{-E_1/T}) + \chi_{\alpha 02}^{\mathrm{Pr}}(1 - e^{-E_2/T}) \tag{3}$$

$$+ (C_{\mathrm{Pr}}(2J+1)/T - \chi_{\alpha 01}^{\mathrm{Pr}}E_1/T - \chi_{\alpha 02}^{\mathrm{Pr}}E_2/T)e^{-E_2/T}]/Z.$$

Here, the Fe subsystem is described by the Curie–Weiss law and, for the Pr^{3+} ions, we use a simplified expression for the susceptibility in the crystal field in which E_1 and E_2 represent the energies of the first excited level and the center of gravity of all the other excited states of the principal multiplet ${}^3H_4$ of the Pr^{3+} ion ($J = 4$), respectively; the quantities $\chi_{\alpha 01}^{\mathrm{Pr}}$ and $\chi_{\alpha 02}^{\mathrm{Pr}}$ determine the contribution of the magnetic dipole transitions between the ground state and the aforementioned excited states; $Z = 1 + e^{-E_1/T} + (2J - 1)e^{-E_2/T}$; $C_{\mathrm{Fe,\,Pr}}$ are the Curie–Weiss constants; and the subscript α is z, $\perp$. Expression (3) takes into account the main features of the rare-earth subsystem at both high and low temperatures. The results of calculations allow us to adequately describe the experiment (Fig. 1) and to determine the characteristic parameters of the Pr^{3+} ion in the crystal field: $E_1 \approx 55$ K, $E_2 \approx 550$–650 K, $\chi^{Pr}_{z02}/\chi^{Pr}_{z01} \approx 2.5$, and $\chi^{Pr}_{\perp 02}/\chi^{Pr}_{\perp 01} \approx 0$. Here, the susceptibility values at $T = 0$, i.e., $\chi^{Pr}_{\alpha 0} = \chi^{Pr}_{\alpha 01} + \chi^{Pr}_{\alpha 02}$, where $\alpha = z, \perp$, were taken from the experiment; the Curie–Weiss constants $C_{Fe,\,Pr}$ were determined by their theoretical values; and the paramagnetic Curie temperature $\theta_{Fe} \approx 130$ K was taken to be equal to that known for $YFe_3(BO_3)_4$ [7].

Now, let us consider the magnetoelectric properties of $PrFe_3(BO_3)_4$ and analyze them by taking into account the characteristic features of the ground state of the Pr ion. According to the ferroborate symmetry, which is determined by the $R32$ space group and the transformation properties of the antiferromagnetic vector $\mathbf{l}$ of the Fe subsystem and magnetic moments $\mathbf{m}_i$ ($i = 1, 2$) of the R subsystem, the electric polarization can be represented in the form [3]

$$P_x = c_1 l_y l_z + c_2(l_x^2 - l_y^2) + \frac{1}{2}\sum_{i=1}^{2}[c_3(m_{ix}^2 - m_{iy}^2) + c_4 m_{iz} H_y + c_5 m_{iz} M_{iy}], \tag{4a}$$

$$P_y = -c_1 l_x l_z - 2c_2 l_x l_y - \frac{1}{2}\sum_{i=1}^{2}[2c_3 m_{ix} m_{iy} + c_4 m_{iz} H_x + c_5 m_{iz} m_{ix}], \tag{4b}$$

$$P_z = c_6 l_x l_z(l_x^2 - 3l_y^2) + \frac{1}{2}\sum_{i=1}^{2} c_7 m_{ix} m_{iz}(m_{ix}^2 - 3m_{iy}^2), \tag{4c}$$

where c_1, c_2, …, and c_7 are the magnetoelectric constants. At the spin-flop transition induced by the field $H \parallel c$, one should primarily expect polarization jumps along the a and b axes: $\Delta P_x \sim c_2(l_x^2 - l_y^2) + \frac{1}{2}\Sigma_i c_3(m_{ix}^2 - m_{iy}^2)$ and $\Delta P_y \sim -2c_2 l_x l_y - \frac{1}{2}\Sigma_i 2c_3 m_{ix} m_{iy}$, respectively, which are caused by the appearance of x or y components of the vectors $\mathbf{l}$ and $\mathbf{m}_i$ in the basal plane. In this case, owing to the specificity of the ground state of the Pr component, m_{ix} and m_{iy} are only determined by its Van Vleck susceptibility $\sim\chi_\perp^{VV} H_{ex}$. The amplitude of the jump and its sign essentially depend on the orientation of the magnetic moments in the basal plane in the spin-flop phase. Therefore, the increase in the electric polarization along the a axis that was observed in the experiment after the transition to the spin-flop phase (Fig. 4a) may be related to this jump if the vectors $\mathbf{l}$ and $\mathbf{m}_i$ are reoriented toward either the a (x) axis or the b (y) axis.

Another feature of the polarization behavior that is associated with the field dependence of polarization in the region $H_z < H_{sf}$ and manifests itself as a small peak in the field corresponding to the spin-flop transition H_{sf} (Fig. 4) may be related to the contributions of $l_x l_z$, $l_y l_z$, $m_{ix} m_{iz}$, $m_{iy} m_{iz}$, $H_x m_{iz}$, and $H_y m_{iz}$ to expressions (4a) and (4b). They can become nonzero because of small deviations of the magnetic field from the c axis in actual experimental conditions, which leads to deviations of magnetic moments from the c axis in the fields $H < H_{sf}$. The modeling performed by us showed that the contributions proportional to $l_x l_z$ and $l_y l_z$ first quadratically depend on the magnetic field and reach their maximum amplitude values near H_{sf}; then, in the fields $H > H_{sf}$, they decrease. The behavior of the polarization along the b axis that was observed in the experiment (Fig. 4b) is likely to be governed by these contributions, because the polarization jump (as for ΔP_x) did not manifest itself in this case, presumably because of the predominant spin orientation along either the a axis or the b axis in the spin-flop phase, in which this jump is equal to zero.

Finally, we note one more feature in the behavior of the polarization along the a axis: this feature manifests itself in the form of a noticeable polarization decrease in the fields above H_{sf} (Fig. 4a). A possible origin of this anomaly is the spin reorientation in the basal plane due to the "parasitic" x or y components of the magnetic field. Such polarization anomalies were observed in easy-plane ferroborates $NdFe_3(BO_3)_4$ [3], $YFe_3(BO_3)_4$, and $EuFe_3(BO_3)_4$ [7] at the point of the spin reorientation to the direction perpendicular to the field in fields of ~7–8 kOe applied in the basal plane.

The field dependences of the electric polarization obtained for the magnetic field applied in the basal plane are adequately described by the expression $P_b = C_3 m_x^2 = C_3(\chi_\perp^{Pr} H_x)^2$, i.e., are determined by the contribution of the Pr subsystem. The inset in Fig. 5 shows the temperature dependence of the experimentally determined coefficient C_3^{Pr}, which multiplies the quadratic term in the field and corresponds to the longitudinal polarization along the a axis, and (the solid line) the dependence $C_3^{Pr} = C_3(\chi_\perp^{Pr})^2$ calculated with the same parameters that were used for describing the transverse susceptibility of praseodymium (Fig. 1). One can see that the calculated curve is in reasonable agreement with the experimental data. A more rigorous consideration of the temperature dependences of the electric polarization requires the calculation of multipole moments, the inclusion of which may lead to an even better agreement between theory and experiment.

CONCLUSIONS

Thus, our studies of $PrFe_3(BO_3)_4$ allowed us to reveal the important role of the rare-earth subsystem in the formation of the magnetic and magnetoelectric properties of this material. The characteristic feature of the Pr^{3+} ion is the singlet character of its ground state. The latter determines the nonzero initial susceptibility in the uniaxial phase and the linear behavior of the magnetization curves both above and below the field corresponding to the spin-flop transition, in contrast to the case of $TbFe_3(BO_3)_4$ [4, 8], where the quasi-doublet splitting in the crystal field is equal to zero. The anisotropy of the magnetic susceptibility of Pr^{3+} and the Pr–Fe exchange stabilize the uniaxial magnetic structure. The analysis allowed us to quantitatively describe the main experimental results and to determine the key parameters of the ground state of the Pr^{3+} ion (the splitting in the crystal field and the magnitude of the exchange field). We showed that the electric polarization anomalies observed at the spin-flop transition are very sensitive to the details of the magnetic structure and the magnetic field orientation, which can be used for obtaining additional information on the magnetic structure, in particular, on the spin orientation in the spin-flop phase.

We are grateful to A.K. Zvezdin and A.P. Pyatakov for useful discussions. This work was supported by the Russian Foundation for Basic Research (project no. 07-02-00580).

REFERENCES

1. A. N. Vasil’ev and E. A. Popova, Fiz. Nizk. Temp. **32**, 968 (2006).
2. A. K. Zvezdin, S. S. Krotov, A. M. Kadomtseva, et al., Pis’ma Zh. Eksp. Teor. Fiz. **81**, 335 (2005) [JETP Lett. **81**, 272 (2005)].
3. A. K. Zvezdin, G. P. Vorob’ev, A. I. Kadomtseva, et al., Pis’ma Zh. Eksp. Teor. Fiz. **83**, 600 (2006) [JETP Lett. **83**, 509 (2006)].
4. A. M. Kadomtseva, Yu. F. Popov, G. P. Vorob’ev, et al., *1st International Interdisciplinary Symposium Multiferroics-2007: Media with Structural and Magnetic Ordering*.
5. M. N. Popova, E. P. Chukalina, T. N. Stanislavchuk, and L. N. Bezmaternykh, Izv. Ross. Akad. Nauk, Ser. Fiz. **70**, 1652 (2006).
6. L. N. Bezmaternykh, S. A. Kharlamova, and V. L. Temerov, Kristallografiya **49**, 1 (2004).
7. V. Yu. Ivanov, A. A. Mukhin, A. M. Kuzmenko, et al., *International Conference Functional Materials ICFM-2007, Ukraine, Crimea, Partenit, October 1–6, 2007*, p. 207.
8. E. A. Popova, D. V. Volkov, A. N. Vasiliev, et al., Phys. Rev. B **75**, 224413 (2007).

Translated by E. Golyamina